Supplementary information file for

Rapid voltage sensing with single nanorods via the quantum confined Stark effect

Omri Bar-Elli[*], Dan Steinitz[*], Gaoling Yang[*], Ron Tenne[*], Anastasia Ludwig[§], Yung Kuo[+], Antoine Triller[§], Shimon Weiss[+‡], Dan Oron[*]

Details of the collection setup

As explained in the methods section, a dichroic mirror is used to split the emission spectrum of a single nanorod (NR) into two independent detectors. Figure 3b of the main text illustrates the importance of splitting the spectrum in half or as close as possible. Due to size variations between NRs their emission peak is shifted with respect to one another. To overcome this issue, we designed a tunable wavelength beam splitter. Dichroic mirrors are dielectric filters composed of thin layers of materials with different refractive indices. Each surface introduces a reflected wave and the interference of the reflection sums up into a wavelength dependent reflection coefficient. Owing to this design, the transmission (and reflection) spectrum of dichroic mirrors is sensitive to the angle of incidence of impinging light. After testing the angle dependence of several dichroic mirrors, we deduced that the cutoff wavelength is inversely proportional to the angle of incidence and surmised a rule of thumb whereby a change of ~1nm in the cutoff wavelength is achieved by ~1^0 change in the angle of incidence. Thus, increasing the angle of incidence by 1^0 will result in a ~1nm blue shift in the cutoff wavelength. When we attempted to blue shift the cutoff for more than ~5^0, the transmission spectrum changed dramatically, while achieving a red shift proved easier and did not change the transmission spectrum significantly even when changing the angle of incidence by ~-15^0.

Details of the nanorods synthesis

ZnSe/CdS core-shell NCs was synthesized following a previously published procedure with some modifications.[1]

Chemicals

Hexadecylamine (HAD, 98%, Aldrich), diethylzinc (Et_2Zn, 1 M solution in hexane, Aldrich) Cadmium oxide (99.99%, Aldrich), Sulfur (99.999%, Aldrich), Selenium (99.999%, Aldrich), oleic acid (OA, 90%, Aldrich), trioctylphosphine (TOP, 90%, Aldrich), dodecylamine (98%, Fluka), trioctylphosphine oxide (TOPO, technical grade, 99% Aldrich), 1-octadecene (ODE, technical grade, 90% Aldrich), hexadecylamine (HPA, 99%, Aldrich), n-octadecylphosphonic acid (ODPA, 99%, PCI), methanol (anhydrous, 99.8%, Aldrich), hexane (anhydrous, 99.9%, Aldrich), toluene (99.8%, Aldrich). All chemicals were used as received without any further purification.

Synthesis of ZnSe NCs: 9.4 g of hexadecylamine was degassed under vacuum at 120 °C in a reaction flask, under argon flow, the mixture was heated up to 310 °C. Then, a mixture of 1 mL 1.0 M selenium dissolved in trioctylphosphine, 0.8 mL diethylzinc and 4 mL

trioctylphosphine, was quickly injected. The reaction was continued at a constant temperature of 270 °C for 25 min and then cooled to room temperature.

Preparation of Cadmium and Sulfur Stock Solutions. 0.034 M cadmium oleate was prepared by mixing 0.03 g (0.24 mmol) CdO in 0.6 mL oleic acid and 6.4 mL ODE. The solution was heated to 280 °C under argon flow with rigorous stirring until all of the CdO dissolved. 0.29 M S solution was prepared by adding 23.3 mg sulfur in 2.5 mL of dodecylamine at ~40 °C.

CdS Shell Synthesis. For typical CdS shell coating, 1.1 g unprocessed ZnSe cores, 5.3 mL octadecene (ODE) were loaded into a 50 mL three-neck flask. The solution was degassed at 100 °C. After that the solution was heated to 240 °C under argon, a mixture of 0.6 mL of 0.034 mmol/mL cadmium oleate stock solution and 0.06 mL of 0.29 mmol/mL sulfur stock solution was injected continuously at 0.72 mL/h. After the injection was finished, the mixture was further annealed for 5 min at 240 °C and then cooled down to room temperature.

ZnSe/CdS-CdS NRs Synthesis. This synthesis was adapted from the previously reported procedure in the literature.[2,3] In a typical synthesis CdO (60 mg), ODPA (290 mg) and HPA (80 mg) are mixed in TOPO (3.0 g). The mixture is degassed under vacuum at 150 °C for 90 min. After degassing step, the solution was heated to 380 °C under argon until it became clear, then 1.8 mL of TOP was injected and the temperature was recovered to 380 °C. Subsequently a solution of 120 mg S in 1.8 mL TOP mix with 40 nmol ZnSe/CdS nanocrystals is rapidly injected. Concentration of the ZnSe/CdS solution was estimated by the extinction at 436nm through a 1cm cuvette.[4] Then the growth was stopped after nanorods grow for 8 min at 365 °C. The NRs were precipitated with methanol and dispersed in toluene.

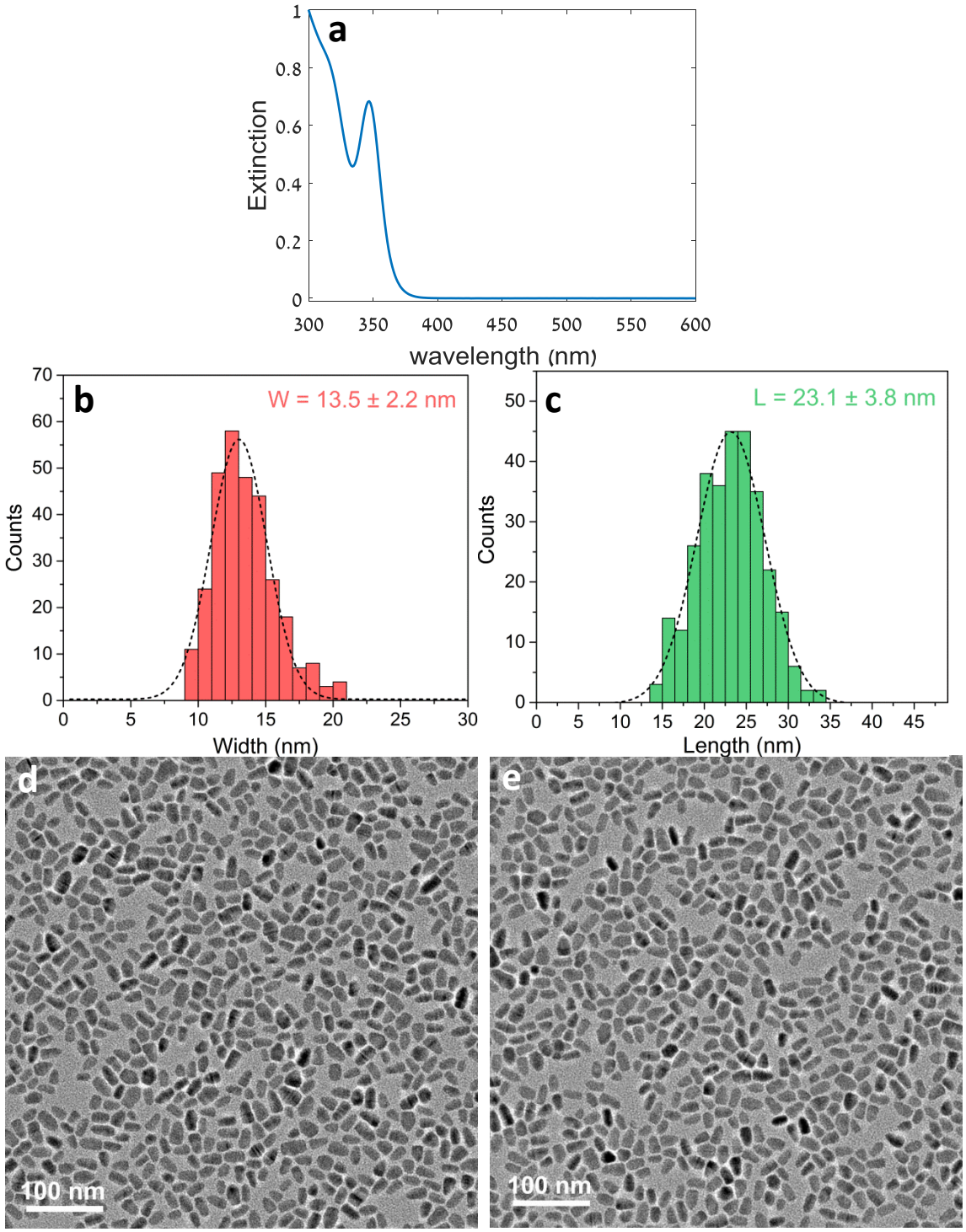

Figure S1 – (a) Extinction spectrum of ZnSe seeds. (b) width size distribution of the ZnSe/CdS NRs. (c) length size distribution of the ZnSe/CdS NRs. (d) and (e) TEM images of the final NRs.

NR's size was determined using ImageJ sampling over 200 different NRs and fitting a Gaussian to the histograms.

Details of the analysis

The blinking histogram is used to determine a threshold in order to eliminate dark "off" state periods from the QCSE response analysis.

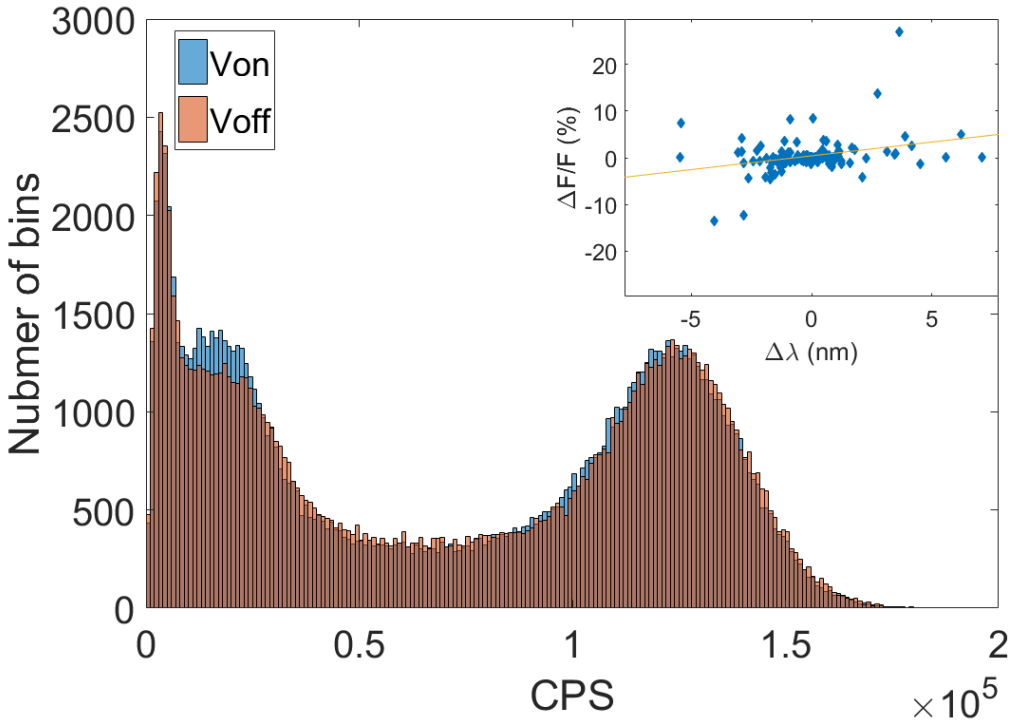

Figure S2 – Example of a histogram over the blinking trace separated into V_{on} an V_{off} periods, it is clear this particle exhibits a small (-0.7%) intensity decrease as a response to the applied voltage. Inset shows a correlation between the intensity change and spectral shift.

The NR orientation may be estimated by rotating a polarizer in the detection channel. Since the NR emission is somewhat polarized a maximum signal would be measured when the polarizer is aligned with the NR. Doing this we estimated the orientation of 6 NR. Figure S3 depicts this data, where a correlation between the orientation and the spectral shift is seen.

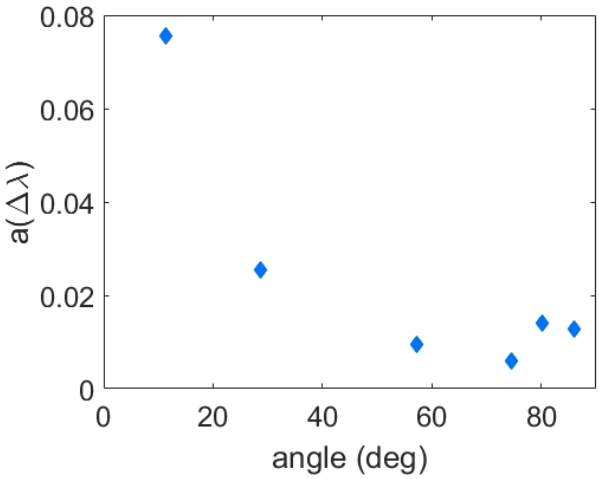

Figure S3 – The spectral shift estimator (a) as a function of particle orientation in the electric field from 6 different particles. 0 degrees indicate a NR parallel to the electric field.

An example of the QCSE spectral shift dependence on the applied electric field:

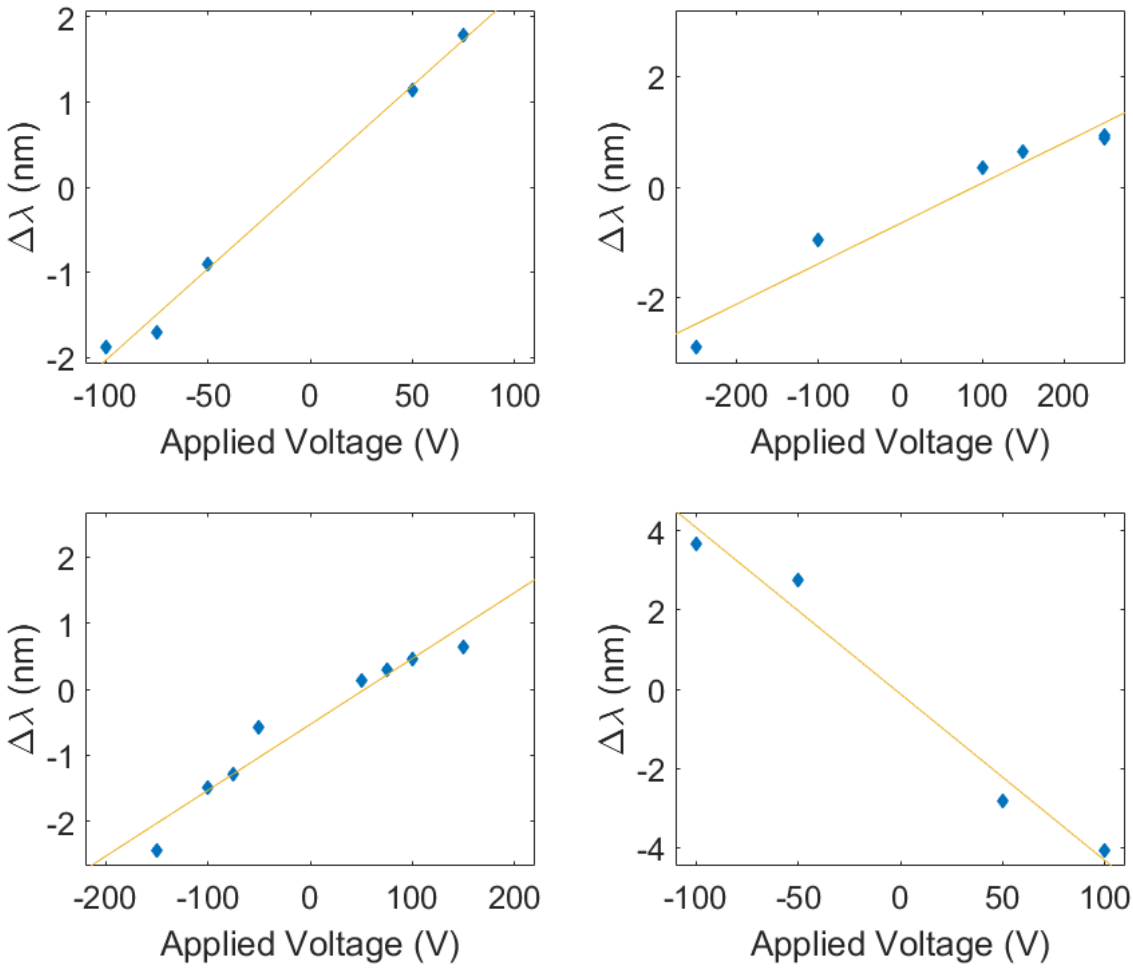

Figure S4 – 4 examples of single particles exhibiting a linear dependence of the spectral shift on the external electric field applied. A linear trend line is provided as a guide.

Determining whether a spectral shift occurred due to QCSE does not require specific knowledge of the dichroic cutoff wavelength, nor does it require a simulation for comparison. These are provided here as methods for unit conversion from the chosen unit-less estimator to nanometers. The conversion enables comparison of our results with previous work in the field, as the common and intuitive way to quantify the spectral shift is in nanometers or meV.

Estimating the spectral shift in nanometers by comparing real measurements to simulation requires two main assumptions. First, the transmission and reflection spectrum of the dichroic mirror used to split the emission peak is approximated by a step function with zero loss. The mirror's cutoff wavelength is taken from the measured spectrum of the dichroic. The transmission spectrum of the dichroic measured at a specific angle of incidence is given in Figure S1a together with a step function at 604nm. One can appreciate this approximation is reasonable. Second, the emission spectrum is approximated by a Gaussian function, the width of which is taken from measured single particle spectra (Fig. 2d).

Since this model may be written analytically it is possible to numerically solve. An alternative approach is to generate the objects in simulation and calculate from them the desired quantities. The analytic approach is described here in detail.

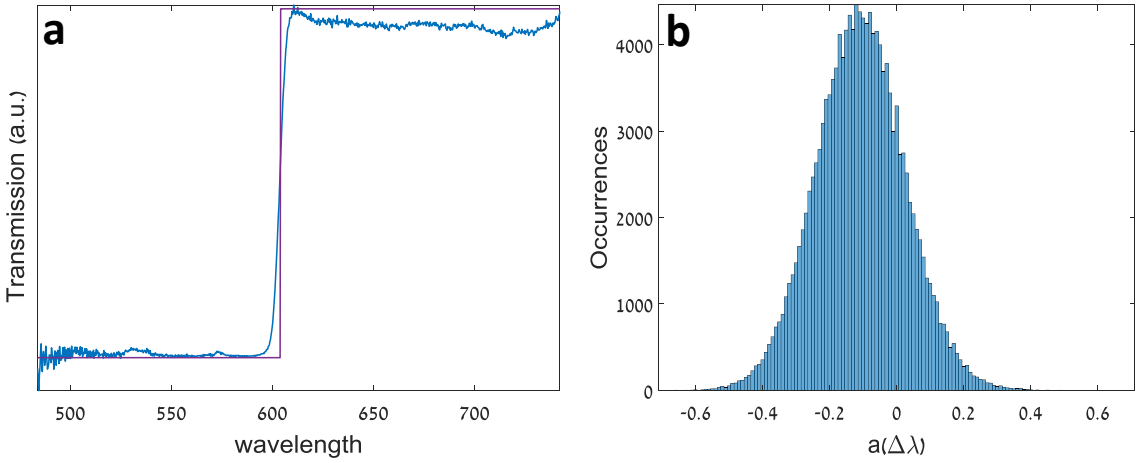

Figure S5 – (a) Transmission spectrum of the dichroic used in the detection setup at a specific angle of incidence and a step function at 604nm. (b) A histogram of the shift estimator with binning of the voltage cycle period (1ms), the mean of the distribution is taken as the shift estimator reported in Figure 3c and the standard deviation is taken as the error for the Allan deviation analysis.

From the measured data, we extract the quantity $a_i = \frac{t_i}{t_i + r_i}$ separately from time bins when no voltage was applied (*0*) and those in which voltage was applied (*V*). Where, t_0 and r_0 are respectively the transmitted and reflected intensity when no voltage was applied and t_V and r_V are the same but for periods in which a voltage was applied. To relate this estimator to wavelength in nanometers we define:

$$g_0(x) = \frac{N}{\sigma\sqrt{2\pi}} e^{-\frac{(x-x_0)^2}{2\sigma^2}}, \quad g_V(x) = \frac{N}{\sigma\sqrt{2\pi}} e^{-\frac{(x-x_V)^2}{2\sigma^2}}$$

Where *x* is the wavelength, g_0 and g_V are the Gaussian emission spectrum when no voltage was applied (g_0) and when voltage was applied (g_V), with central wavelengths x_0 and x_V respectively, N is the amplitude of the Gaussian corresponding to the intensity or, number of photons. σ, the standard deviation of the Gaussian function, is estimated from single particle spectra and set to 25nm. This is likely a minor overestimation of the width since single particle spectra require long exposures making broadening by spectral diffusion evident. We estimated the broadening of the Gaussian due to spectral diffusion as ~5nm on the time scale of the spectrum acquisition time. While this broadening may skew the results, its small contribution renders it negligible.

We further define $f(x)$ as the step function approximating a dichroic mirror with a cutoff wavelength x_s:

$$f(x)=\begin{cases}0 & x<x_s\\ 1 & x>x_s\end{cases}$$

Thus we can calculate the intensity of transmission and reflection from the dichroic:

$$r_i=\int_{-\infty}^{\infty}\left(1-f(x)\right)g_i(x)\,dx=\int_{-\infty}^{x_s}g_i(x)\,dx$$

$$t_i=\int_{-\infty}^{\infty}f(x)\,g_i(x)\,dx=\int_{x_s}^{\infty}g_i(x)\,dx$$

Substituting and solving in the definition for a_Δ:

$$a_\Delta=\frac{t_V}{r_V+t_V}-\frac{t_0}{r_0+t_0}=\frac{1}{N}\left(\int_{x_s}^{\infty}g_V(x)\,dx-\int_{x_s}^{\infty}g_0(x)\,dx\right)=$$

$$=\frac{1}{2}\left(erfc\left(\frac{x_s-x_1}{\sqrt{2}\sigma}\right)-erfc\left(\frac{x_s-x_0}{\sqrt{2}\sigma}\right)\right)$$

To extract the spectral shift $\left(\Delta\lambda=x_1-x_0\right)$ in nanometers one needs to estimate a_0 as well. Substituting in the definition for a_i and solving for x_0 (for simplicity we assume $I_V=I_0$):

$$a_0=\frac{t_0-r_0}{I_0}=1-erfc\left(-\frac{x_s-x_0}{\sqrt{2}\sigma}\right)$$

$$\Rightarrow x_0=x_s+\sqrt{2}\sigma erfc^{-1}\left(1-a_0\right)$$

Extracting the difference:

$$\Delta x=\sqrt{2}\sigma\cdot\left(erfc^{-1}\left(2a_0\right)-erfc^{-1}\left(2\left(a_\Delta+a_0\right)\right)\right)$$

The dichroic cutoff defines the sensitivity by influencing a_V and a_0, as the shifts take the emission central wavelength away from the dichroic cutoff the sensitivity is diminished; this is illustrated in Figure 3b.

Using the experimental data, we extract a Δx value for each time bin of 0.5ms to get a series of values for x_0 and x_V. In the main text we present an estimator for the shift and not for the separate central wavelengths since it is not necessary to convert these results to nanometers for the purpose of detecting an applied voltage.

Error estimation

We present here the error estimation for the estimator presented in the main text for the spectral shift. Note, that the effects of spectral diffusion are neglected in this calculation. Assuming shot noise as the only noise source, that is: $\Delta t=\sqrt{t}$ and $\Delta r=\sqrt{r}$, and using the error propagation formula, we describe the error in the estimator:

$$\Delta a_{\Delta} = \sqrt{\left(\Delta t_V \frac{\partial a}{\partial t_V}\right)^2 + \left(\Delta r_V \frac{\partial a}{\partial r_V}\right)^2 + \left(\Delta t_0 \frac{\partial a}{\partial t_0}\right)^2 + \left(\Delta r_0 \frac{\partial a}{\partial r_0}\right)^2}$$

Since intensity changes due to voltage are mostly negligible, and for simplicity, we assume: $\Delta F = 0 \Rightarrow I_V = I_0$:

$$\Delta a_{\Delta} = \sqrt{\frac{1}{I^3}\left(t_V r_V + t_0 r_0\right)} = \frac{1}{\sqrt{I}} \sqrt{\alpha_V(\lambda)\left(1-\alpha_V(\lambda)\right) + \alpha_0(\lambda)\left(1-\alpha_0(\lambda)\right)}$$

Where $\alpha_i(\lambda) = \frac{r_i}{I}$ is a constant. From here we see that the error in *a(Δλ)* scales as $N^{-0.5}$, where N is the number of photons. This is used to calculate the error shown in Figure 3d by setting N according to the count rate in the measurement.

It is important to note that bins are averaged over only if they are found consecutively in the "on state". For this reason, NRs exhibiting fast transitions with few prolonged "blink on" periods would have insufficient statistics for extended averaging.

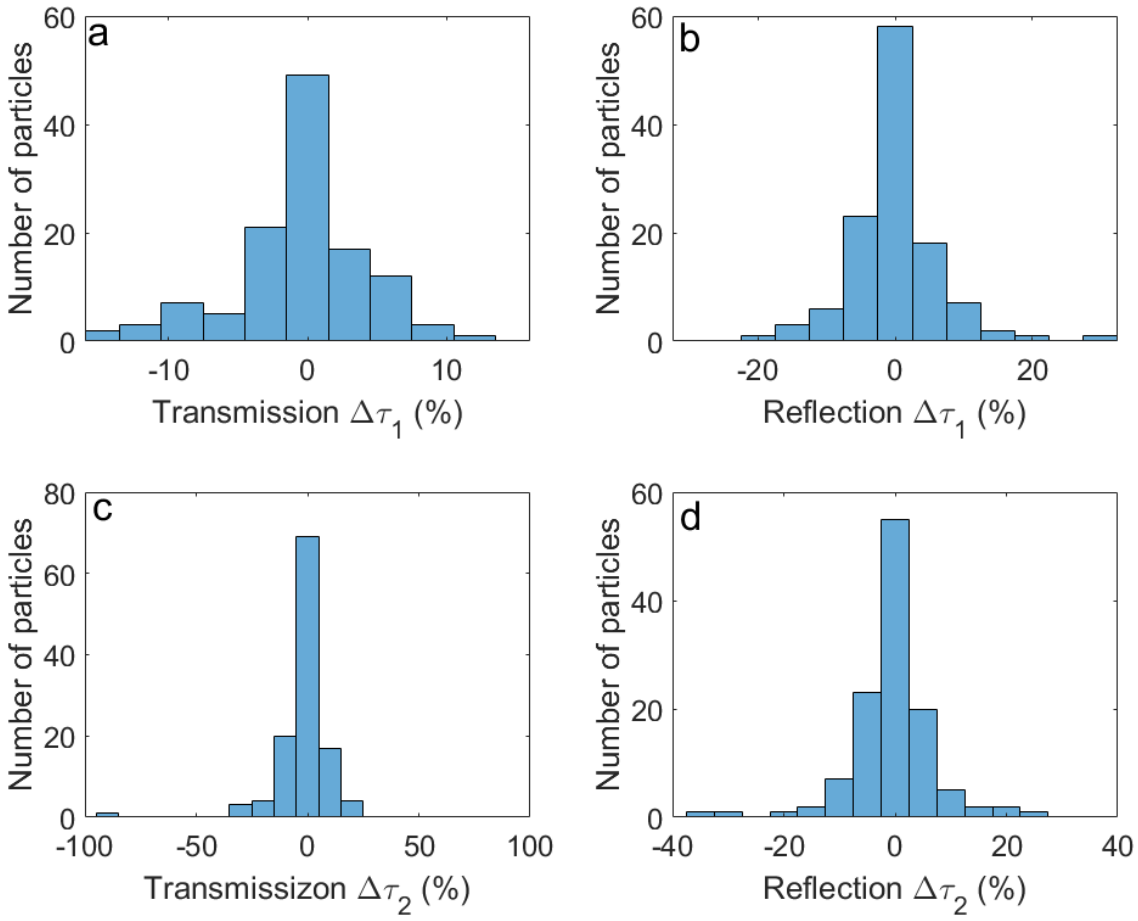

Figure S6 – Histograms of the relative lifetime variations. $\Delta\tau_1$ and $\Delta\tau_2$ refer, respectively, to the short and long lifetime components. Transmission and reflection refer to the detection channel.

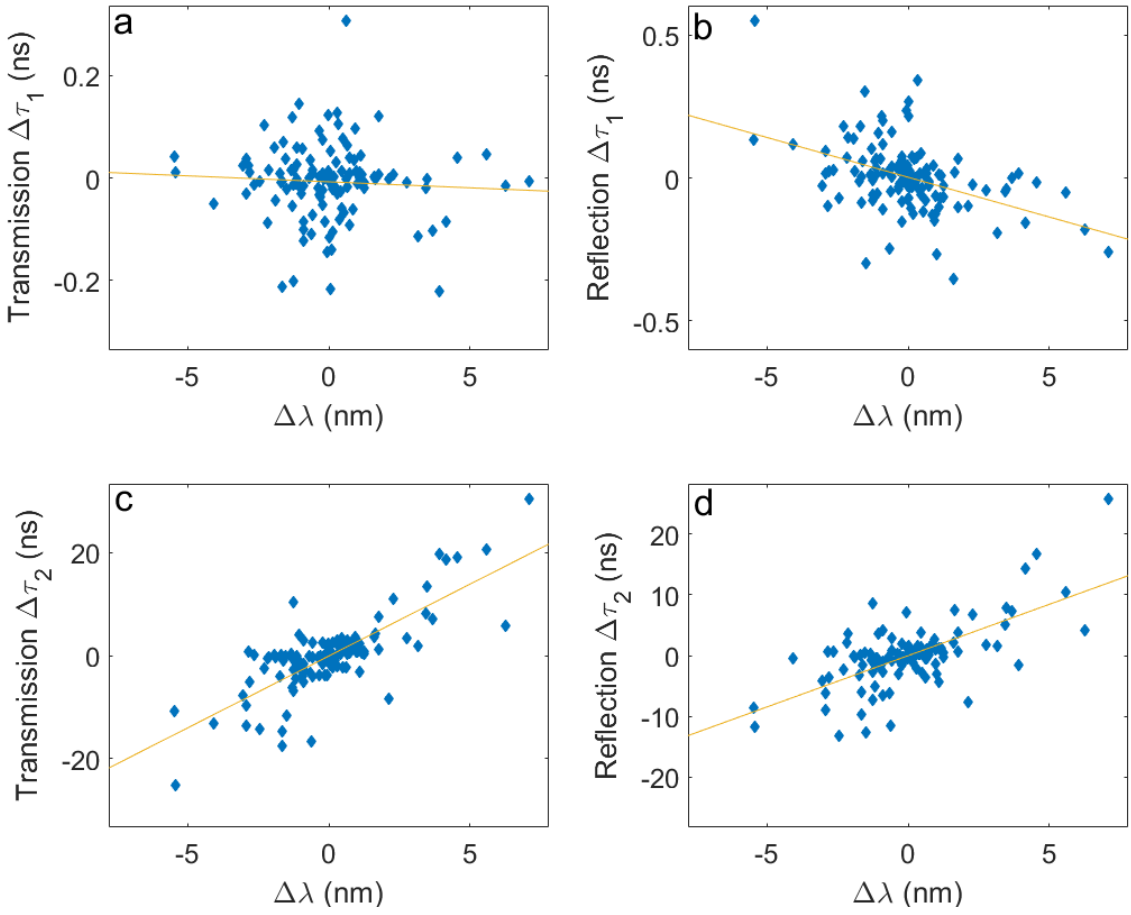

Figure S7 – Scatter plots depicting the correlation between lifetime variations and spectral shifts due to QCSE. $\Delta\tau_1$ and $\Delta\tau_2$ refer, respectively, to the short and long lifetime components. Transmission and reflection refer to the detection channel.

The apparent negative correlation between the short lifetime and the spectral shift likely occurs due to the nature of the decay mechanism leading to the existence of such a lifetime. An applied electric field may enhance the efficiency of such a decay mechanism leading to an even larger decay constant and shorter lifetime.

Details of the microelectrode fabrication process

The electrodes were designed using Layout Editor. A mask was prepared on using standard chromium on soda lime-glass substrate (Nanofilm) exposed in a laser-writer (Heidelberg instruments, µPG 101).

Cover slips were immersed and washed with acetone, isopropyl alcohol (IPA), and distilled water, dried under a nitrogen stream and left for 5min on a hot plate at 150^0C. Photoresist (Shipley, S1813) was spin coated at 2000RPM with a 1000 (RPM/s) ramp for 40sec followed by a soft bake of 60sec at 115^0C. Exposure was done using the prepared mask and a mask aligner (Karl Suss, MA 6/BA 6) Development (Shipley, MF319) was performed for 55sec followed by washing with copious amounts of distilled water. The cover slips were further

treated using O_2 plasma ashing (Diener Electronics Pico-DHP.) A thin adhesion layer of ~3nm of Cr was evaporated onto the substrates using an evaporator (Selene ODEM), subsequently Au was evaporated to yield any desired thickness in the range of 150-300nm. A chilling mechanism was activated during the Cr deposition. Liftoff was done in acetone for 1 hour and mild brief sonication. Resulting in inter-electrode gap of 2.5-4.5µm.

Table S1 - summary of the measured NRs

NR#	Electrode gap* (µm)	Voltage (V)	Electric Field** (kV/cm)	Intensity*** (cps)	Δλ (nm)	Channel 1 Δτ (ns)	Channel 2 Δτ (ns)
1	3.5	100	285	3.53E+04	-2.3	-2.5	-2.4
2	3.5	100	285	6.67E+04	-0.6	-16.7	-11.5
3	3.5	100	285	1.02E+05	3.9	19.8	-1.5
4	3.5	100	285	1.37E+05	2.1	-8.3	-7.8
5	3.6	100	275	6.09E+04	-5.4	-25.2	-11.7
6	3.8	100	267	4.92E+04	0.6	-2.3	-3.6
7	4.1	100	243	5.37E+04	-1.2	10.4	8.6
8	4.1	100	243	4.04E+04	0.5	-2.3	-2.9
9	4.1	100	243	4.07E+04	0.6	2.7	-0.5
10	4.1	100	243	4.56E+04	4.5	19.1	16.6
11	4.1	100	243	6.52E+04	7.1	30.4	25.7
12	4.1	100	243	3.27E+04	3.4	8.2	5.0
13	4.2	100	236	3.49E+04	-0.9	-5.1	-6.5
14	4.1	100	243	5.16E+04	-1.3	-0.6	-0.8
15	4.2	100	236	8.57E+04	-1.3	-2.8	-2.7
16	4.0	100	251	3.89E+04	0.1	-0.5	0.3
16	4.0	100	251	4.74E+04	0.0	-0.2	1.7
17	4.0	100	251	5.44E+04	0.0	-0.1	0.4
18	4.0	100	251	3.67E+04	0.0	0.5	-0.5
19	4.0	100	251	7.69E+04	-0.3	-3.8	-3.0
20	4.1	100	243	1.62E+05	-2.2	-0.6	2.2
20	4.1	100	243	9.47E+04	-1.1	3.9	3.6
21	4.1	100	243	6.88E+04	3.5	13.4	7.9
22	4.1	100	243	5.82E+04	4.2	18.8	14.2
23	4.1	100	243	6.73E+04	-0.6	-3.4	-6.1
24	4.1	100	243	5.15E+04	1.0	2.0	1.1
25	4.1	100	243	4.58E+04	0.7	1.6	0.7
26	4.1	100	243	3.51E+04	-1.1	-1.6	-1.3
27	4.1	100	243	4.82E+04	-5.5	-10.8	-8.6
28	4.0	100	251	6.84E+04	-0.6	-0.3	-0.8
29	3.8	50	133	1.46E+05	-1.1	-0.9	-0.4
29	3.8	-50	-133	1.39E+05	1.2	0.5	1.2
29	3.8	75	200	1.37E+05	-2.6	0.0	0.7

30	3.9	50	129	7.89E+04	0.0	0.6	0.2
31	3.9	50	129	8.74E+04	-1.3	0.2	0.3
32	3.6	50	138	8.30E+04	-1.3	-6.8	-7.3
33	3.6	50	138	3.73E+04	-1.5	-0.1	0.4
33	3.6	50	138	3.29E+04	-1.9	0.0	-0.1
34	3.8	50	133	1.50E+05	0.7	0.9	0.8
35	3.6	50	138	1.60E+05	-0.4	-0.4	0.2
36	3.6	50	138	1.30E+05	0.2	-0.5	-1.2
37	3.8	50	133	2.79E+05	1.1	2.3	1.3
38	3.8	50	133	1.21E+05	-0.1	-3.8	-0.7
38	3.8	-50	-133	1.11E+05	0.0	-0.8	1.5
39	3.6	50	138	1.34E+05	1.6	3.7	2.1
39	3.6	-50	-138	9.67E+04	-1.6	-0.9	-1.6
40	3.6	50	138	1.67E+05	-1.1	-0.2	-0.5
41	3.8	50	133	2.03E+05	0.1	0.0	0.1
42	3.8	50	133	1.32E+05	-0.2	-0.2	-0.3
43	3.8	50	133	1.28E+05	1.8	7.5	3.7
44	3.8	50	133	1.53E+05	-1.2	-4.5	-5.0
45	4.1	50	122	2.52E+05	0.4	0.5	0.4
45	4.1	75	182	2.27E+05	0.5	1.4	0.8
46	4.1	50	122	1.14E+05	1.0	0.9	-3.0
47	4.2	50	118	1.37E+05	1.1	1.2	1.0
47	4.2	-50	-118	1.08E+05	-0.9	-1.7	-1.1
47	4.2	75	177	1.34E+05	1.8	1.2	0.6
47	4.2	-75	-177	1.11E+05	-1.7	0.0	0.2
47	4.2	-100	-236	5.94E+04	-1.9	-0.3	-0.3
48	4.1	-100	-243	1.31E+05	-2.8	-5.0	-3.6
48	4.1	100	243	1.33E+05	6.2	5.8	4.2
48	4.1	50	122	9.18E+04	3.2	1.9	1.6
49	4.0	50	125	1.43E+05	-0.2	-1.5	-1.6
50	4.0	50	125	1.68E+05	-0.9	-2.7	-2.8
51	4.0	50	125	1.60E+05	1.7	4.3	7.5
52	3.8	50	133	2.08E+05	-1.7	-4.1	-3.3
53	3.9	50	129	1.62E+05	-0.2	-0.9	-1.5
54	3.9	50	129	8.46E+04	0.0	2.3	1.1
55	3.9	50	129	1.90E+05	0.4	3.3	3.7
56	3.9	50	129	1.54E+05	-0.4	-0.6	-0.7
57	3.9	50	129	1.40E+05	-0.7	-0.1	-0.2
58	3.9	50	129	8.01E+04	-0.2	-1.2	-0.9
59	3.9	50	129	6.99E+04	0.1	-2.3	0.1
60	4	250	625	1.33E+05	0.9	3.2	1.7
60	4	-250	-625	6.08E+04	-2.9	-13.7	-8.9
60	4	150	375	6.35E+04	0.7	3.0	1.1

60	4	250	625	7.87E+04	0.9	3.6	2.8
60	4	100	250	1.05E+05	0.3	1.9	1.5
60	4	-100	-250	1.28E+05	-0.9	-4.0	-1.3
61	4	-75	-188	4.03E+04	-1.3	-6.1	-0.7
61	4	75	188	3.50E+04	0.3	3.0	1.0
61	4	150	375	2.83E+04	0.6	0.4	-0.5
61	4	-150	-375	7.95E+04	-2.4	-14.3	-13.3
61	4	-100	-250	7.91E+04	-1.5	-11.6	-12.8
61	4	100	250	4.55E+04	0.5	2.2	1.4
61	4	50	125	1.52E+05	0.1	2.4	0.3
61	4	-50	-125	1.02E+05	-0.6	-4.1	0.9
61	4	0	0	8.62E+04	-0.1	-3.9	7.1
61	4	-200	-500	1.08E+05	-1.7	-14.7	-6.0
61	4	200	500	2.80E+05	0.1	-1.0	-0.5
62	4.2	100	238	1.93E+05	-1.7	-17.6	-9.8
63	4.2	100	238	3.25E+05	1.0	0.8	-1.4
63	4.2	-100	-238	3.34E+05	-0.2	2.4	2.0
63	4.2	100	238	4.15E+05	0.2	-1.0	-0.1
63	4.2	50	119	3.46E+05	0.1	0.6	-0.7
64	4	100	250	7.43E+04	-2.1	-0.3	3.7
64	4	-100	-250	1.79E+05	1.3	0.4	-0.3
65	4	-100	-250	9.76E+04	5.6	20.6	10.5
66	4.2	-100	-238	1.14E+05	-0.9	3.0	4.2
67	4.2	100	238	1.85E+05	-1.1	-2.2	-1.5
68	4.2	100	238	1.43E+05	1.1	-3.2	-4.3
69	4.2	100	238	7.49E+04	-2.9	-9.7	-6.3
70	4.2	100	238	8.74E+04	-3.0	-7.7	-4.1
71	4.2	100	238	4.16E+04	-4.1	-13.2	-0.5
71	4.2	-100	-238	4.30E+04	3.7	7.1	7.3
71	4.2	-50	-119	3.88E+04	2.7	3.4	1.8
71	4.2	50	119	4.72E+04	-2.8	0.9	0.7
72	5.4	-50	-93	1.16E+05	0.2	-0.2	0.1
73	5.4	-50	-93	2.54E+05	0.8	3.0	1.9
73	5.4	50	93	2.41E+05	0.0	-1.9	0.2
74	5.4	50	93	9.33E+04	0.0	1.3	-0.3
75	5.4	50	93	1.01E+05	-1.0	-2.8	-2.2
76	4.4	-50	-114	3.52E+05	-0.6	2.4	2.9
76	4.4	50	114	3.93E+05	0.3	-2.0	-2.1
77	4.4	50	114	1.99E+05	0.7	0.6	0.1
78	4.4	50	114	1.62E+05	0.4	0.2	0.3
79	4.4	50	114	1.89E+05	-0.3	-0.1	0.1
80	4.4	50	114	1.79E+05	-0.3	-0.3	-0.2

81	4.4	50	114	2.08E+05	1.2	0.7	0.4
82	4.4	50	114	1.14E+05	2.3	11.0	6.7

*Measurement error of the electrode gaps is ±0.15µm

**Estimated by approximation to an ideal plate capacitor.

***The average intensity during periods that pass the "off state" intensity threshold.

References

(1) Tyrakowski, C. M.; Shamirian, A.; Rowland, C. E.; Shen, H.; Das, A.; Schaller, R. D.; Snee, P. T. *Chem. Mater.* **2015**, *27* (21), 7276–7281.

(2) Dorfs, D.; Salant, A.; Popov, I.; Banin, U. *Small* **2008**, *4* (9), 1319–1323.

(3) Carbone, L.; Nobile, C.; De Giorgi, M.; Sala, F. Della; Morello, G.; Pompa, P.; Hytch, M.; Snoeck, E.; Fiore, A.; Franchini, I. R.; Nadasan, M.; Silvestre, A. F.; Chiodo, L.; Kudera, S.; Cingolani, R.; Krahne, R.; Manna, L. *Nano Lett.* **2007**, *7* (10), 2942–2950.

(4) Yu, W. W.; Qu, L.; Guo, W.; Peng, X. *Chem. Mater.* **2003**, *15* (14), 2854–2860.